Model development of a new single room ventilation enthalpy exchanger under wet conditions

A. Parthoens[1]*, S. Gendebien[2], P. Lemaitre[3], V. Lemort[4]

[(1),(2),(4)] Université de Liège, Belgium

[(3)]Certech, Belgium

1. ABSTRACT

The present paper deals with the model development of an enthalpy exchanger under wet conditions in the frame of single room ventilation. Numerous models take into account simultaneous heat and vapour transfer, but not liquid transfer. This new model takes into account condensation on stale air side, liquid transfer through porous membrane and finally water evaporation on the fresh air side. The involved phenomena depend on each other as the evaporation cools down the membrane, intensifying condensation. A coupling is then necessary, leading to spatial discretization of the exchanger and numerical considerations. An experimental set-up has been used to validate the membrane mass transfer model. The enthalpy exchanger model is then used to simulate performances under different outdoor conditions.

Keywords: Enthalpy exchanger, heat recovery, liquid water recovery

2. INTRODUCTION

2.1 Context

In the frame of energy savings, buildings (new and refurbished) are getting more and more thermally insulated and airtight. As outside air infiltrations are prevented due to the building envelope, ventilation systems are required to ensure a sufficient indoor air quality (Händel, 2001). The relative part of ventilation in the global building consumption is then increasing (Roulet et al., 2001). To fulfill the air renewal, different systems exist, going from simple natural ventilation to more complex systems with heat recovery. The heat recovery allows to decrease the ventilation energy losses by the means of a heat exchanger. Furthermore, beside the sensible heat, it is needed to ensure a good humidity level in the fresh air. This leads to a latent load representing a non-negligible part of the required air conditioning energy (Nasif et al., 2010). To reduce this load, devices that are called enthalpy exchanger, may be implemented to recover humidity in addition to heat.

2.2 State of art

Many works in scientific literature handle these kinds of exchangers. Dugaria et al. (2015) predicted with a 2-dimensional finite difference model sensible, latent and total effectiveness sensibility to membranes' characteristics. Sebai et al. (2014) modelled cross-flow enthalpy exchangers with balanced or unbalanced flow with a control volume method. Zhang (2009) measured latent effectiveness going up to about 70% with a paper-plate and paper-fin exchanger. Niu & Zhang (2001) showed numerically and experimentally the effectiveness evolution of enthalpy exchangers for different membranes and operating conditions. Koester et al. (2017) developed and validated a CFD model of what they called a counter- cross-flow enthalpy exchanger, presenting thermal as well as hydraulic performances of such an exchanger. They reached thermal and latent effectiveness of respectively 95 and 80% for most

advantageous tested conditions. Liang (2014) measured experimentally performances of a parallel-plates enthalpy exchanger. He showed that sensible effectiveness was independent of the relative humidity. However the latent effectiveness increased with it. Many more works are available in the literature and Zeng et al. (2017) made a review of such devices for building applications.

2.3 Motivations

All these publications show the real interest of these enthalpy exchangers. However most of these works consider membranes that are generally fragile such as paper. These are efficient considering heat and mass transfer but cannot be thermoformed and their lifetime is quite short. Furthermore, to the best authors' knowledge, no modelling of liquid water through a membrane exists. This paper tries to fulfill this gap by introducing a new model of liquid water transfer through a porous membrane in the frame of air-to-air enthalpy exchangers. The mass transfer model through the membrane is validated with a specific thermoformed polymer membrane and the simulation results of an enthalpy exchanger are presented for membranes of different permeability.

3. MODEL DESCRIPTION

The wet regime model handles several different aspects. There are first the heat transfer phenomena, with convection between the wall and the air fluxes as well as conduction within the wall. Then, different kinds of mass transfer are considered: moisture condensation in the stale air side as the air is cooled down, liquid water transfer through the membrane due to water partial pressure difference and finally evaporation of this water in the fresh air stream. It is to note that the different phenomena are linked. As the water film evaporates in the fresh air, it induces cooling of the membrane. If the membrane cools down, the condensation process will be intensified.

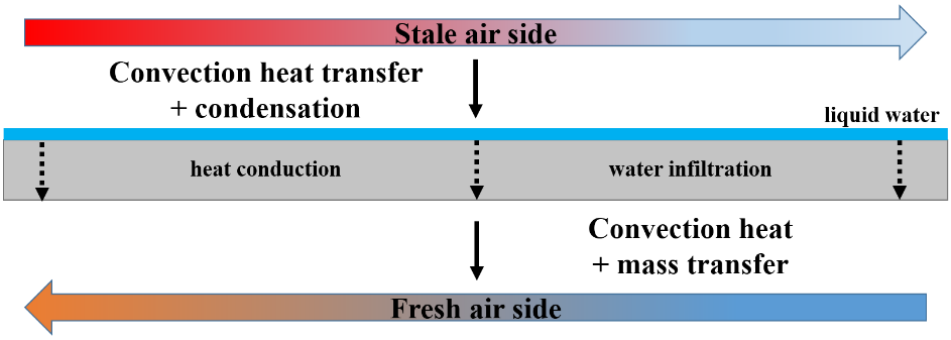

Figure 1: Schematic representation of the membrane and of the main physical phenomena

The global model links different bricks that take into account each of the phenomena. Each of these blocks is described hereafter.

3.1 Convection heat transfer and condensation on the stale air side

While the conditions are such that the stale air cools down when going through the exchanger, the partial pressure of vapour increases. If this pressure reaches the saturation pressure, condensation takes place. The modeling of this process was described and experimentally validated by Gendebien et al. (2013). It is a simplified cooling coil model based on the work of Lebrun et al. (1990), Brandemuehl et al. (1993) and Morisot & Marchio (2002). From this model, the mass flowrate of condensates $\dot{M}_{cond}$ as well as the heat transfer rate can be

evaluated. Lebrun et al. (1990) demonstrated that the total heat transfer rate could be expressed as:

$$\dot{Q}_{tot,st} = \varepsilon_{st} \cdot \dot{C}_{st,fict} \cdot (T_{su,wb,st} - T_{su,f}) \quad (1)$$

with ε_{st} being the effectiveness of the ε-NTU method and

$$\dot{C}_{st,fict} = \dot{M}_{st} \frac{h_{su,st} - h_{ex,st}}{T_{su,wb,st} - T_{ex,wb,st}} \quad (2)$$

This cooling coil model allows to determine the conditions at the outlet of the coil, the amount of condensates but it does not deal with mass transfer through a membrane. To be consistent, adaptations need to be implemented. The latter ones are explained in a following section

3.2 Water and heat transfer through the membrane

As porous membrane is wetted by the condensates, liquid water infiltrates up to the fresh air side. This mass transfer is driven by the difference of the water partial pressure on both sides of the membrane. This relies on two main assumptions:

- The whole system is in steady state,
- The porous membrane is already filled with liquid water (capillary effect is neglected).

As it is a liquid flow through a porous media, an equivalent law of Darcy was used, involving a membrane resistance R and a partial water pressure difference.

$$\dot{M}_{w,memb,th} = \frac{\Delta P \cdot A_{wet} \cdot \rho}{R \cdot \mu \cdot \delta} \quad (3)$$

with

$$\Delta P = P_{w,sat}(T_{memb,st}) - P_{w,f} \quad (4)$$

The membrane resistance is a feature of the membrane and should be experimentally determined. Nasif et al. (2012) showed that the membranes could be classified in three different categories. First the membrane resistance (to vapour, not liquid) can be independent of the atmospheric conditions. For the two other categories, the resistance can either increase or decrease with the air humidity ratio. In the frame of this paper, the resistance is considered as constant. The mass flow rate expressed in (3) is a maximum threshold and if the quantity of water available to migrate through the membrane is smaller, it must be taken into account. The water that actually goes from one side of the membrane to the other is then the minimum between the flow rate expressed in (3) and the condensed water flow rate:

$$\dot{M}_{w,memb} = \min(\dot{M}_{cond}, \dot{M}_{w,memb,th}) \quad (5)$$

The heat transfer through the membrane was described using the conduction heat transfer equations with the assumption that the conductivity only depends on the membrane material and not on the water quantity in the membrane. This hypothesis makes sense if the porosity is relatively low and if the membrane is thin. The liquid water reaching the fresh air side is now subject to evaporation.

3.3 Evaporation on the fresh air side

The liquid film arising from the membrane to the fresh air side is confronted to an air stream. A gas in motion in contact with a liquid leads to convective effects. This mass transfer between the wet surface and the air stream was modeled following the Ashrae Handbook (1977) formalism. The driving force of the water transfer is the humidity ratio difference:

$$\dot{M}_{w,ev,f,th} = h_{mass} \cdot A_{wet} \cdot (\omega_{memb,f} - \overline{\omega}_f) \quad (6)$$

where $\omega_{memb,f}$ is the specific humidity at the membrane level (as there is a liquid film, the air is considered as saturated), $\overline{\omega}_f$ the mean humidity ratio of the fresh air flow and $h_m$is the mass convective coefficient. h_m was computed using the Chilton-Coburn analogy (Nasif et al. 2012):

$$h_{mass} = \frac{h}{\overline{cp}_a} \cdot Le^{-1/3} \quad (7)$$

The Lewis number was set to 1 as the Prandtl and Schmidt numbers are close to the unity for gas mixtures (Keys & Crawford, 1980). Iteration loops were made to predict the fresh air exhaust conditions to deduce the mean specific heat coefficient and humidity ratio, allowing to compute the mass convective transfer coefficient. Similarly to (5), the effective evaporated mass rate is expressed as:

$$\dot{M}_{w,ev,f} = \min(\dot{M}_{w,ev,f,th}, \dot{M}_{w,memb}) \quad (8)$$

The latent heat corresponding to this water evaporation can be written as:

$$\dot{Q}_{lat,f} = \dot{M}_f \cdot h_{fg} \cdot (\omega_{ex,f} - \omega_{su,f}) \quad (9)$$

with h_{fg} being the latent heat of vaporization being set to 2.442 kJ/kg. The sensible heat transfer can be computed from two different ways:

$$\dot{Q}_{sens,f,1} = \varepsilon_f \cdot \dot{C}_{min} \cdot (T_{su,st} - T_{su,f}) \quad (10)$$

$$\dot{Q}_{sens,f,2} = \dot{M}_f \cdot cp_f \cdot (T_{ex,f} - T_{su,f}) \quad (11)$$

The total heat exchange rate on the fresh air side is the sum of the latent and sensible heat flow rates.

3.4 Coupling and discretization

The equations described until here are consistent independently, however, the influence of the evaporation on the fresh air side on the condensation on the stale air side was not taken into account. To fix this, a slight modification of the equations was introduced. The trick used was to consider, for the heat transfer only (not for the mass transfer), the membrane as a fictitious wall that is at a constant temperature. In this formalism, the two air streams are not exchanging heat with each other but with this wall. If the ambient losses are neglected, the idea is applying the energy conservation by iterating on the wall temperature $T_{wall,fict}$ in order to equal the total heat transfer on both sides. The equations (1) and (10) then become:

$$\dot{Q}_{sens,f,1} = \varepsilon_f \cdot \dot{C}_f \cdot (T_{wall,fict} - T_{su,f}) \quad (12)$$

$$\dot{Q}_{tot,st} = \varepsilon_{st} \cdot \dot{C}_{st,fict} \cdot (T_{su,wb,st} - T_{wall,fict}) \quad (13)$$

ε_f and ε_{st} are the effectiveness of respectively the fresh and the stale air side of the ε-NTU method, now considering a semi-isothermal exchanger. As the quantity of evaporated water

Eq. (6) impacts the latent Eq.(9) and thus the total heat transfer rate on the fresh air side, it will impact the wall temperature Eq. (12), which will impact the stale air side Eq. (13). The coupling is therefore made.

However, considering this technique at the whole exchanger level, the stale and the fresh air cannot exit the exchanger at a temperature respectively lower and higher than the fictitious wall temperature, leading again to an inconsistency. This is why a spatial discretization of the exchanger had to be made.

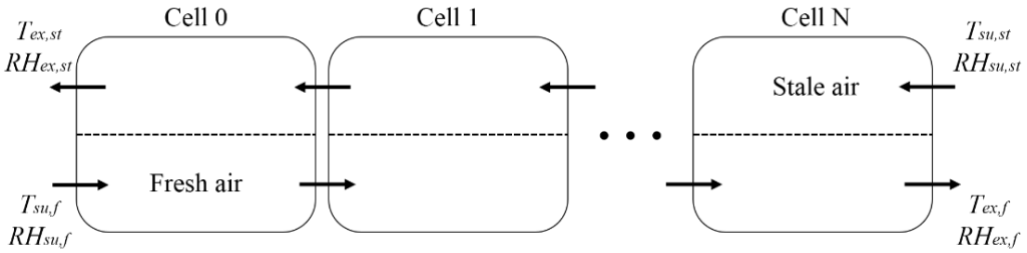

Figure 2: Representation of the special discretization of the enthalpy exchanger

The model described before was applied to each cell and the inputs of the cell *i* are:

$$x_{su,f}[i] = x_{ex,f}[i-1] \quad (14)$$

$$x_{su,st}[i] = x_{ex,st}[i+1] \quad (15)$$

x being either the temperature or the humidity. Guesses on the supply conditions of each cell are made on one side of the exchanger and the model iterates until the convergence of each cell is reached.

3.5 Parametric study of the required number of cells

As the model needs a spatial discretization, the question of the necessary number of cells must be considered. The method envisaged was to draw the model outputs evolution with the number of cells involved. A water resistance tending towards the infinity (i.e. impermeable membrane) was used to compare it with the model without mass transfer validated by Gendebien et al (2015). To see if it is either the number or the size of the cells that is the key parameter, the simulations were done for two exchangers of different sizes. The cells that were considered were are all of the same size fixed with the number of cells. The outputs chosen to check the convergence were the exhaust temperatures and the stale air exhaust humidity.

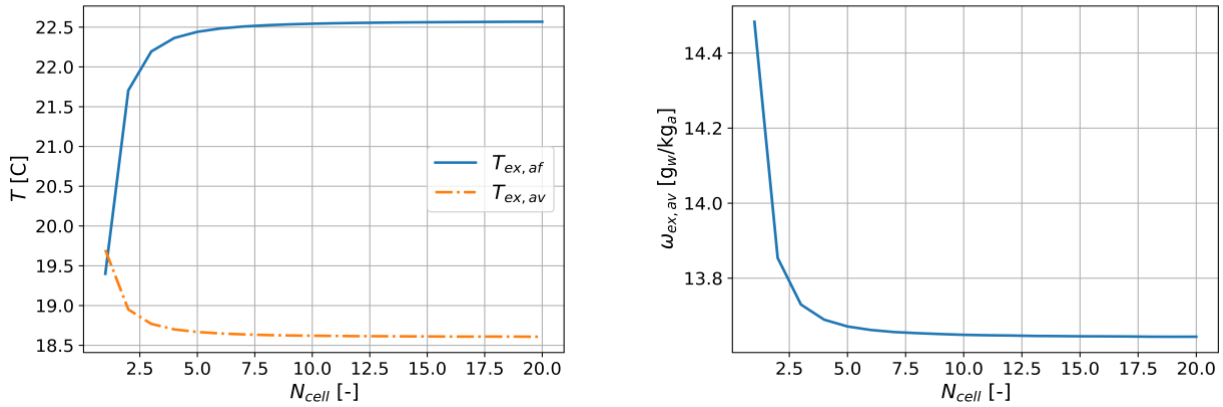

Figure 3: Model outputs versus the number of cells

Obviously, not enough cells will lead to erroneous results. Considering too many cells will lead to a good solution, however the computational time will be much higher. A trade-off should be made to conciliate good results with a reasonable simulation time. Figure 3 suggests that from above 10 cells, refining the discretization will not imply a substantial change in the results. More precisely, Figure 4 shows that from 10 cells, the difference adding new cell is asymptotical to 0. For such an exchanger, using a discretization of 10 cells seems to be the best trade off between the precision the computational time.

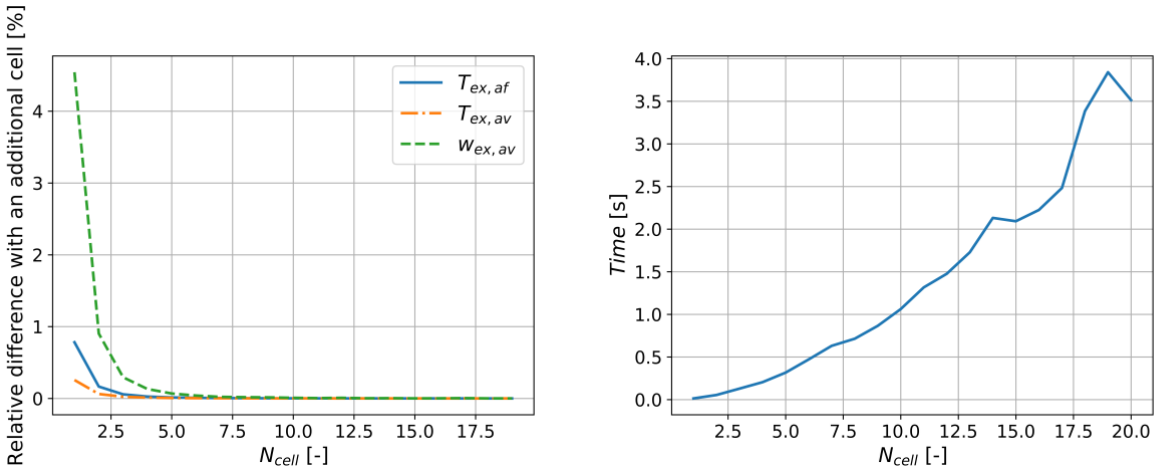

Figure 4: Relative difference of outputs adding a new cell (left) and computational time regarding the number of cell (right)

The simulation time was for simulations conducted with a machine with Intel i7 processor running at 2.5 GHz. The same simulations were achieved for the exact same exchanger and conditions except that rather than having an exchange area of 2 m², it was 4 m². The results showed that the difference of outputs between the 10th and 11th cells was under 0.04%. This revealed that the number of cells is more important than their size. Indeed, for the larger exchanger with the same number of cells, the cells were twice bigger, however, the results were satisfactory. The output difference with the validated model (impermeable) were of 0.40%, 0.72% and 0.70% for respectively $T_{ex,f}$, $T_{ex,st}$ and $\omega_{ex,st}$ considering 10 cells for a 4 m² exchanger.

4. MEMBRANE MODEL VALIDATION

The model validation was achieved in different steps. First, the cooling coil model with condensation developed by Gendebien et al. (2015) had been validated in their paper. Therefore this step is skipped in the frame of this paper.

Then the model of the mass transfer through the membrane was considered. First, the membrane resistance of (3) had to be determined experimentally. The experimental setup is represented in Figure 5.

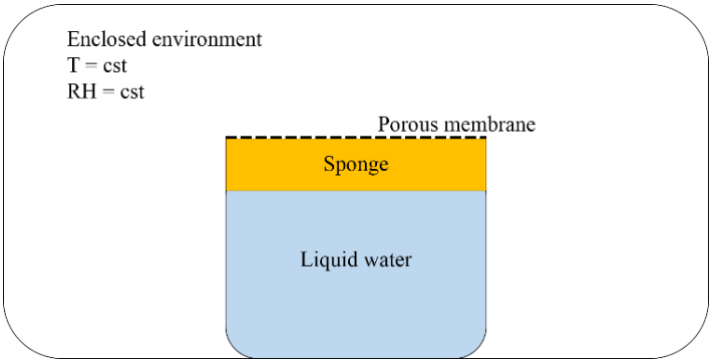

Figure 5: Experimental setup used for the membrane resistance determination

Preliminarily, the membrane was submerged in water for one hour to load all the interstices and to reach steady state conditions. Then, a recipient was filled with liquid water and closed with the membrane. To ensure a permanent contact between the liquid and the membrane, a sponge was added and periodic checks were made to control that the liquid was in contact with the sponge during the whole experiment. This setup was weighted and put in an enclosed environment where the atmospheric conditions were controlled. The temperature was fixed to 23±0.5°C and the relative humidity to 50 ± 1%. After 24 hours in these conditions, the recipient was weighted a second time. The difference between the two measures corresponded to the water that went through the membrane and that was evaporated to the environment. The mass flow rate and the environmental conditions being known, the membrane resistance *R* could be deduced from a rewriting of (4).

Figure 6 represents the normalized mass flow rate of water transferred through the membrane.

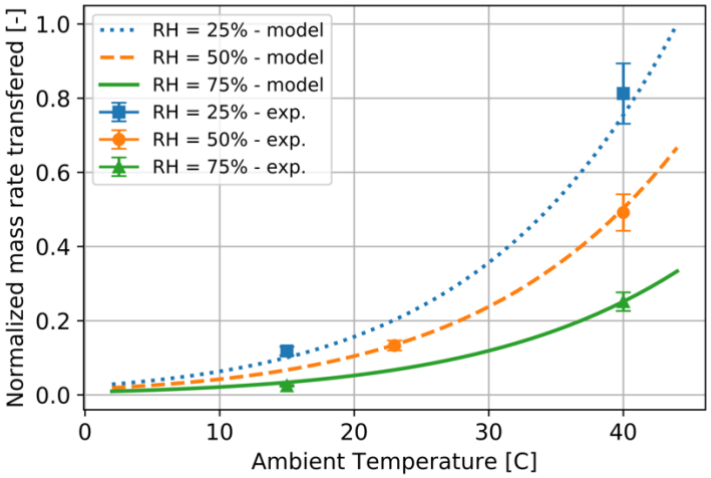

Figure 6: Model validation transfer of water through the membrane

The different curves are the simulation results, varying the temperature and the humidity. If the atmospheric pressure is considered as constant, these two factors totally set the atmospheric conditions. The different markers represent different experimental measurements with a 10% error bar. The membrane resistance was identified with the 40°C and 75% relative humidity point. Figure 6 shows satisfying results for the other points. The membrane model is considered as validated and the assumption of constant membrane resistance (for this specific membrane) is consistent.

5. SIMULATION RESULTS

5.1 Enthalpy exchanger definition

For the simulations, the geometry of the heat exchanger was fixed. A counter-flow exchanger with an exchange surface of 4 m² was considered. This corresponds to an exchanger in single room ventilation units. The design was such that the sensible effectiveness in dry regime with a flow rate of 42 m^3/h is 80%. The thermal conductivity of the membrane was 0.2 W/m/K (i.e. polypropylene) and its thickness was 105 µm.

5.2 Influence of membrane resistance on exchanger effectiveness

The membrane resistance obviously impacts the mass transfer through the membrane for given atmospheric conditions. A parametric study was conducted to see the impact of this

resistance on the sensible and latent effectiveness, for both air flows. The conditions were such that the condensation appears at the inlet of the exchanger (i.e. $RH_{su,st}=100\%$) and at a temperature of 20°C. The fresh air was at 15°C and 80% of relative humidity. Before the analysis, the effectiveness should be defined:

$$\varepsilon_{lat,f} = \frac{\dot{M}_f \cdot h_{fg} \cdot (\omega_{ex,f} - \omega_{su,f})}{\dot{M}_{min} \cdot h_{fg} \cdot (\omega_{su,st} - \omega_{su,f})} \quad (16) \qquad \varepsilon_{lat,st} = \frac{\dot{M}_{st} \cdot h_{fg} \cdot (\omega_{su,st} - \omega_{ex,st})}{\dot{M}_{min} \cdot h_{fg} \cdot (\omega_{su,st} - \omega_{su,f})} \quad (17)$$

$$\varepsilon_{sens,f} = \frac{\dot{C}_f \cdot (T_{ex,f} - T_{su,f})}{\dot{C}_{min} \cdot (T_{su,st} - T_{su,f})} \quad (18) \qquad \varepsilon_{sens,st} = \frac{\dot{C}_{st} \cdot (T_{su,st} - T_{ex,st})}{\dot{C}_{min} \cdot (T_{su,st} - T_{su,f})} \quad (19)$$

$$\varepsilon_{tot,f} = \frac{\dot{M}_f \cdot (h_{ex,f} - h_{su,f})}{\dot{M}_{min} \cdot (h_{su,st} - h_{su,f})} \quad (20) \qquad \varepsilon_{tot,st} = \frac{\dot{M}_{st} \cdot (h_{su,st} - h_{ex,st})}{\dot{M}_{min} \cdot (h_{su,st} - h_{su,f})} \quad (21)$$

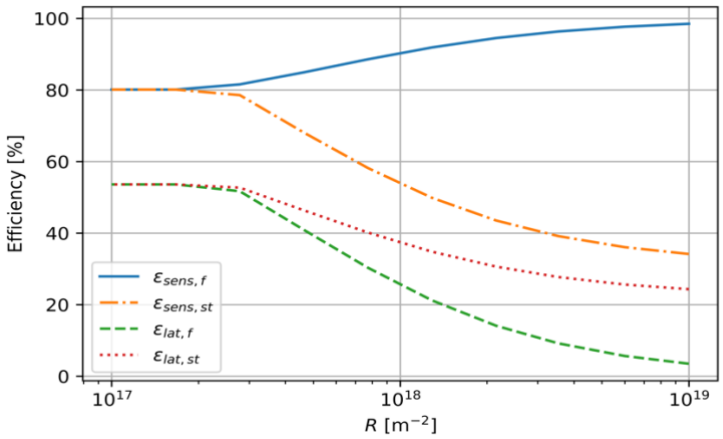

Figure 7: Effectiveness variation regarding the membrane permeability resistance

First, it is to note that for low resistances (high water transfer) constant effectiveness is observed. This means that all the condensed water is transferred through the membrane and evaporated in the fresh air. This case is extreme and should not be considered. Then, as the resistance increases, all effectiveness's decrease, except $\varepsilon_{sens,f}$. This because if less water is transferred and then evaporated, then a larger proportion of the power transferred to the fresh air will be devoted to heating it up. Next, $\varepsilon_{lat,f}$ decreases because if less water is available to evaporate, the exhaust humidity will decrease. Then, if less water evaporates on the fresh air side, the membrane mean temperature will increase. This conducts to a lower sensible heat transfer (smaller temperature difference between the air stream and the membrane) and less condensation as the colder the wall, the higher the condensation. This explains the fall of $\varepsilon_{sens,st}$ and $\varepsilon_{lat,st}$ with the membrane resistance increase.

For the rest of the numerical study, as the resistance is considered constant, it is fixed to a specific value. For the above-mentioned conditions, it was chosen to take a resistance leading to $\varepsilon_{lat,f}$ = 30%, which is consistent with the literature. The matching resistance is R = 7.85E17 m^{-2}.

5.3 Performance mapping

For a deeper understanding of the involved phenomena and coupling of the evaporation and the condensation, different performance maps were drawn, based on simulation results. To build the latter ones, indoor conditions were set to 20°C and 100% HR (to still ensure the condensation from the beginning of the exchanger). Then the outdoor conditions varied from 2 to 18°C and 10 to 90% HR.

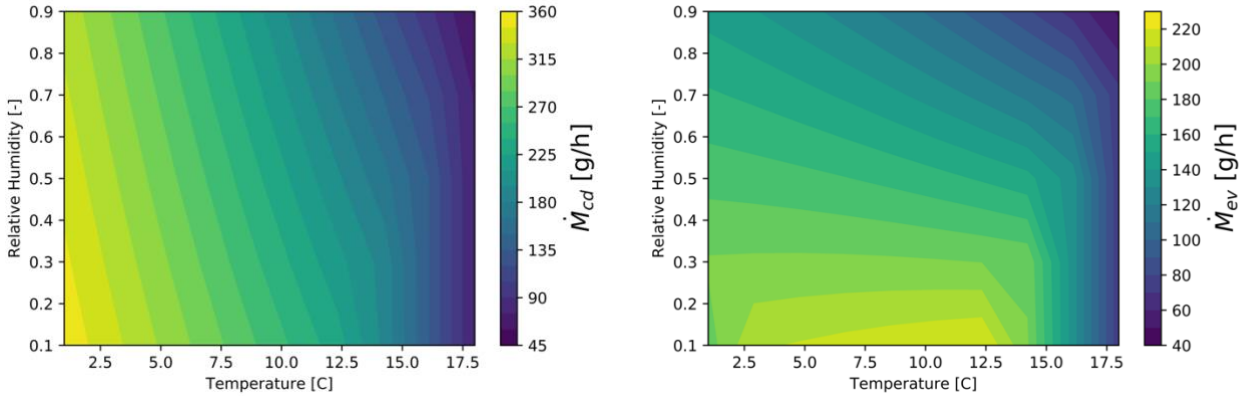

Figure 8: Mass flow rate condensed on the stale air side (left) and evaporated on the fresh air side (right) regarding the fresh air supply temperature and humidity

Looking first at the $\dot{M}_{cd}$ for a constant humidity, the hotter the fresh air, the less the condensation. Intuitively, it is physically consistent. Then for a fixed temperature, the trend is that the condensation is favoured for lower fresh air humidity. If the humidity is low, the water will evaporate more easily, implying a wall cooling.

For a given temperature, as the humidity increases, less water evaporates on the fresh air side. For a fixed humidity, an optimum is observed, resulting on one side on the membrane capacity to transfer water and on the other side on the available quantity of condensates. When the fresh air is cold, it enhances the condensation process. Furthermore, when the air is warmer, the mass transfer is eased but the mass of condensates is limited. The best behaviours result thus from a trade-off.

These phenomena are recovered in the representation of latent effectiveness shown in the next figures. Especially for the fresh air latent effectiveness, the optimum can be easily spotted.

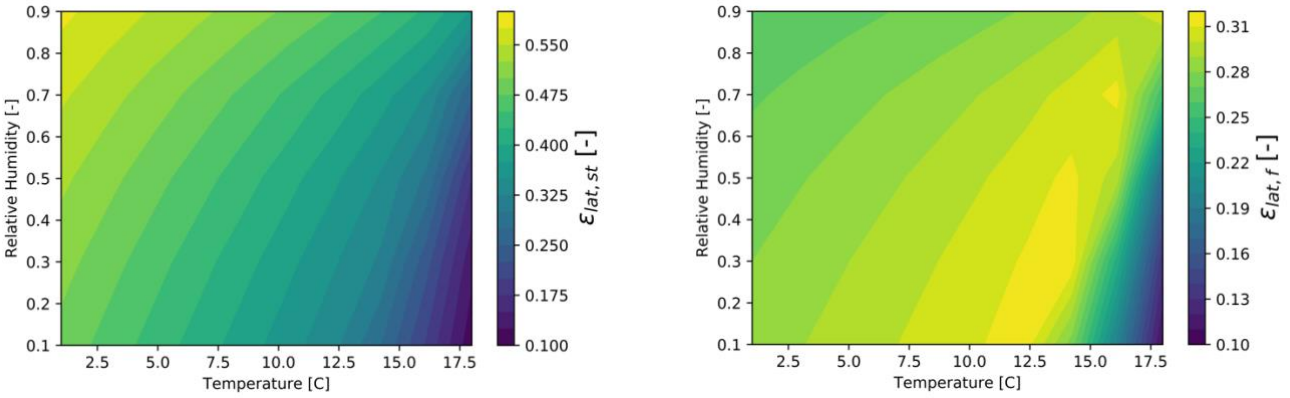

Figure 9: Latent effectiveness (stale air side (left), fresh air side (right)) regarding the outdoor temperature and relative humidity

Then, the sensible effectiveness can be drawn with the same approach.

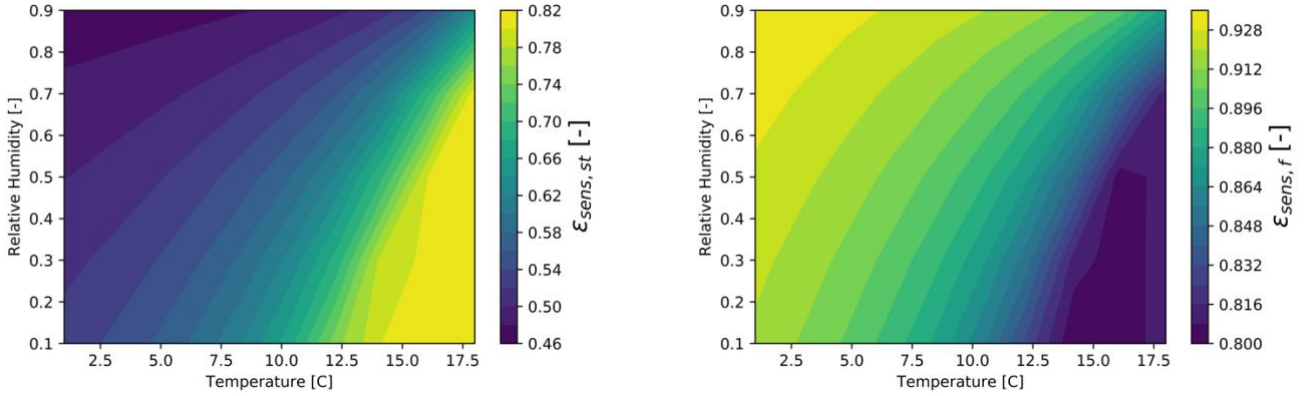

Figure 10: Sensible effectiveness (stale air side (left), fresh air side (right)) regarding the outdoor temperature and relative humidity

For the stale air side, the sensible effectiveness is better while the condensation is low. The combination to have a good sensible effectiveness is hot and dry outdoor air. Hot air limits the condensation and moreover if it is dry, it will enhance evaporation on the fresh air side (giving a colder membrane). Concerning the sensible effectiveness on fresh air side, it is the opposite: it is better for cold and humid air. These conditions are such that the evaporation is limited, leading to a small latent part and thus giving high sensible performances.

To have an idea of the conditions giving a better global heat transfer between the two sides, the same map was drawn for the total heat transfer as well as the total effectiveness (Eq. (20) and (21)).

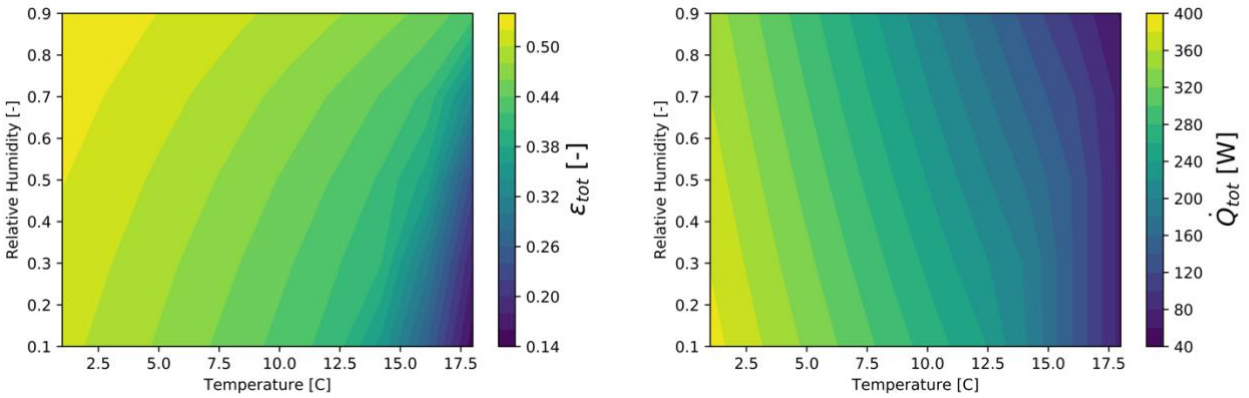

Figure 11: Total effectiveness (left) and total heat transfer (right) regarding the outdoor temperature and relative humidity

To obtain the best total effectiveness, the colder and the more humid the better. A large temperature difference is favourable to high sensible transfer. Then the increase of effectiveness with the humidity can be explained looking at the Eq. (20) and (21). Indeed, for a given temperature, if the supply fresh air humidity is higher, the supply enthalpy will be larger too, decreasing the value of the denominator. Then, to recover a maximum heat power (sensible and latent), the colder and the dryer the best. This combination will lead to a large water condensation on the stale air side and as it is dry, evaporation will be favoured. With the coupling effect, these phenomena will strengthen each other leading to high latent load. Furthermore, with the high temperature difference, the sensible part is also consequent.

6. CONCLUSIONS

This paper attempts to fill a gap in the literature that is the modeling of liquid transfer trough a porous membrane in the frame of air-to-air enthalpy exchangers. The different processes, namely the water condensation, liquid transfer and evaporation were described. As the water evaporation on fresh air side impacts the membrane temperature and thus the condensation process on the stale air side, a coupling between these phenomena was implemented.

The coupling led to the need of special discretization of the enthalpy exchanger to keep physical consistency. The number of cells involved was discussed and it was shown that the number and not the size of the cell was the key parameter. With 10 cells, good numerical results were achieved keeping a reasonable simulation time.

The model of the membrane (not the whole exchanger model) was successfully validated experimentally by measuring the water transfer for different atmospheric conditions

The enthalpy exchanger model under wet conditions was then used to predict the mass transfers, the effectiveness and the exchanged thermal power, for different outdoor conditions. It revealed that to recover maximum heat (sensible and latent), dry and cold conditions are preferred. However to recover a maximum of water in the fresh air flow, an optimum resulting from the ability to transfer water through the membrane and the quantity of condensates available was found.

Acknowledgment

This work was supported by the Walloon Region and the Pole Mecatech [convention 7711].

NOMENCLATURE

QUANTITIES

cp	specific heat capacity, J/kg/K
$\dot{C}$	capacity flowrate, W/K
h	convective coefficient, W/m^2/K or kg/m^2/s
$h_{fg.}$	heat of vaporization, J/kg
Le	Lewis number, -
$\dot{M}$	mass flow rate, kg/s
$\dot{Q}$	heat transfer rate, kg/s
R	membrane resistance, m^{-2}
RH	relative humidity, -

GREEK SYMBOLS

ε	effectiveness, -
δ	thickness, m
Δ	difference, -
ω	specific humidity, kg$_w$/kg$_a$
ρ	density, kg/m^3
μ	dynamic viscosity, Pa.s

7. REFERENCES

Ashrae Handbook. (1977). New-York.

Brandemuehl, M., Gabel, S., & Andersen, I. (1993). A toolkit for secondary HVAC System Energy Calculations. *ASHRAE*.

Dugaria, S., Moro, L., & Del Col, D. (2015). Modelling heat and mass transfer in a membrane-based air-to-air enthalpy exchanger. *33rd UIT (Italian Union of Thermo-fluid-dynamics) Heat Transfer Conference.*

Gendebien, S., Bertagnolio, S., & Lemort, V. (2013). Investigation on a ventilation heat recovery exchanger: Modeling and. *Energy and Buildings, 62*, 176-189.

Händel, C. (2001). Ventilation with heat recovery. *Rheva Journal*.

Keys, W. M., & Crawford, M. E. (1980). *Convective heat and mass transfer* .

Koester, S., Falkenberg, M., Logemann, M., & Wessling, M. (2017). Modeling heat and mass transfer in cross-counterflow enthalpy exchangers. *Journal of Membrane Science*, 68-76.

Lebrun, J., Ding, X., Eppe, J.-P., & Wasac, M. (1990). Cooling Coil Models to be used in Transient and/or Wet Regimes. Theoretical Analysis and Experimental Validation. *Proceedings of SSB*, (pp. 405-411). Liège.

Liang, C. (2014). Experiments Investigation of the Parallel-plates Enthalpy Exchangers. *The 6th International Conference on Applied Energy*, (pp. 2699 – 2703).

Morisot, O., & Marchio, D. (2002). Simplified Model for the Operation of Chilled Water Cooling Coils Under Nonnominal Conditions. *HVAC&R Research*, pp. 135-158.

Nasif, M. S., Al-Waked, R., Behnia, M., & Morrison, G. (2012). Modeling of Air to Air Enthalpy Heat Exchanger. *Heat Transfer Engineering*, 1010-1023.

Nasif, M., AL-Waked, R., Morrison, G., & Behinia, M. (2010). Membrane heat exchanger in HVAC energy recovery systems, systems energy analysis. *Energy and buildings* , 1833-1840.

Niu, J., & Zhang, L. (2001). Membrane-based Enthalpy Exchanger: material considerations and clarification of moisture resistance. *Journal of Membrane Science*, 179-191.

Roulet, C.-A., Heidt, F., Foradini, F., & Pibiri, M.-C. (2001). Real heat recovery with air handling units. *Energy and Buildings, 33*(5), 495-502.

Sebai, R., Chouikh, R., & Guizani, A. (2014). Cross-flow membrane-based enthalpy exchanger balanced and unbalanced flow. *Energy Conversion and Management*, 19-28.

Zeng, C., Liu, S., & Shukla, A. (2017). A review on the air-to-air heat and mass exchanger technologies for building applications. *Renewable and Sustainable Energy Reviews*, 753-774.

Zhang, L.-Z. (2009). Heat and mass transfer in plate-fin enthalpy exchangers with different plate and fin materials. *International Journal of Heat and Mass Transfer*, 2704-2713.